Collective behaviour in two-dimensional cobalt nanoparticle assemblies observed by magnetic force microscopy

VICTOR F. PUNTES*[1], PAU GOROSTIZA[2], DEBORAH M. ARUGUETE[3], NEUS G. BASTUS[1] AND A. PAUL ALIVISATOS[3]

[1]Physics Department, University of Barcelona, 08028 Barcelona, Spain
[2]Department of Molecular and Cell Biology, University of California, Berkeley, Berkeley 94720, USA
[3]College of Chemistry, University of California, Berkeley, Berkeley 94720, USA
*e-mail: vfpuntes@ffn.ub.es

Published online: 28 March 2004; doi:10.1038/nmat1094

The use of magnetic nanoparticles in the development of ultra-high-density recording media is the subject of intense research. Much of the attention of this research is devoted to the stability of magnetic moments, often neglecting the influence of dipolar interactions. Here, we explore the magnetic microstructure of different assemblies of monodisperse cobalt single-domain nanoparticles by magnetic force microscopy and magnetometric measurements. We observe that when the density of particles per unit area is higher than a determined threshold, the two-dimensional self-assemblies behave as a continuous ferromagnetic thin film. Correlated areas (similar to domains) of parallel magnetization roughly ten particles in diameter appear. As this magnetic percolation is mediated by dipolar interactions, the magnetic microstructure, its distribution and stability, is strongly dependent on the topological distribution of the dipoles. Thus, the magnetic structures of three-dimensional assemblies are magnetically soft, and an evolution of the magnetic microstructure is observed with consecutive scans of the microscope tip.

In nanostructured materials built from nanometric units, dipolar interactions play an important role in determining cooperative phenomena at the molecular scale and the final properties of the material[1]. Thus, proximity (matrix) effects, long-range interactions, long-range order, domain walls, hysteresis, collective behaviour, percolation, correlated local and global perturbations and others, are subjects of investigation. Actually, many of these phenomena exhibit striking similarities with other very different systems such as gels, polymers, ceramic superconductors and structural glasses[2,3]. It has been extended to a wide range of other fields, from solids to living organisms and social collectivities[4].

Magnetic nanoparticle compact monolayers have been proposed as suitable for future ultra-high-density magnetic recording media and other technical applications[5,6]. However, it is theoretically well established that in two-dimensional (2D) magnetic systems, the dipolar interactions stabilize long-range magnetic order, and determine the nature and the morphology of such ordered states, which may impede the ability to address a single particle individually in a densely particulate media[7].

In previous work[8], we observed ferromagnetic-like (collective) behaviour in magnetization measurements at low temperature of a 2D self-assembled monolayer of 9-nm-diameter Co particles. Here, we observe by magnetic force microscopy (MFM), large correlated areas in the magnetic structure of 12-nm-diameter ε-cobalt nanoparticle assemblies responsible for the observed ferromagnetic-like behaviour. Previous studies on MFM were focused mainly on magnetic recording media[9] and multidomain magnetic materials[10] as well as on tip characterization[11] and image interpretation[12]. There have been other reports of the imaging and magnetization of Co magnetic dots (with lateral dimensions of 140 × 250 nm, and of 7 nm thickness)[13], iron dots (40 nm thick, 40 to 120 nm diameter)[14] and imaging and magnetic moment estimation of magnetotactic bacteria (50 nm in length and 17.5 nm in radius, if modelled as a cylinder)[15]. The magnetic structure of composites of iron oxide nanoparticles and polymers has been observed[16], and the MFM signal of an individual iron oxide nanoparticle has also been observed[17] without detecting any signal for particles smaller than 15 nm. The magnetic microstructure of individual magnetic nanoparticles has also been observed by Lorentz electron

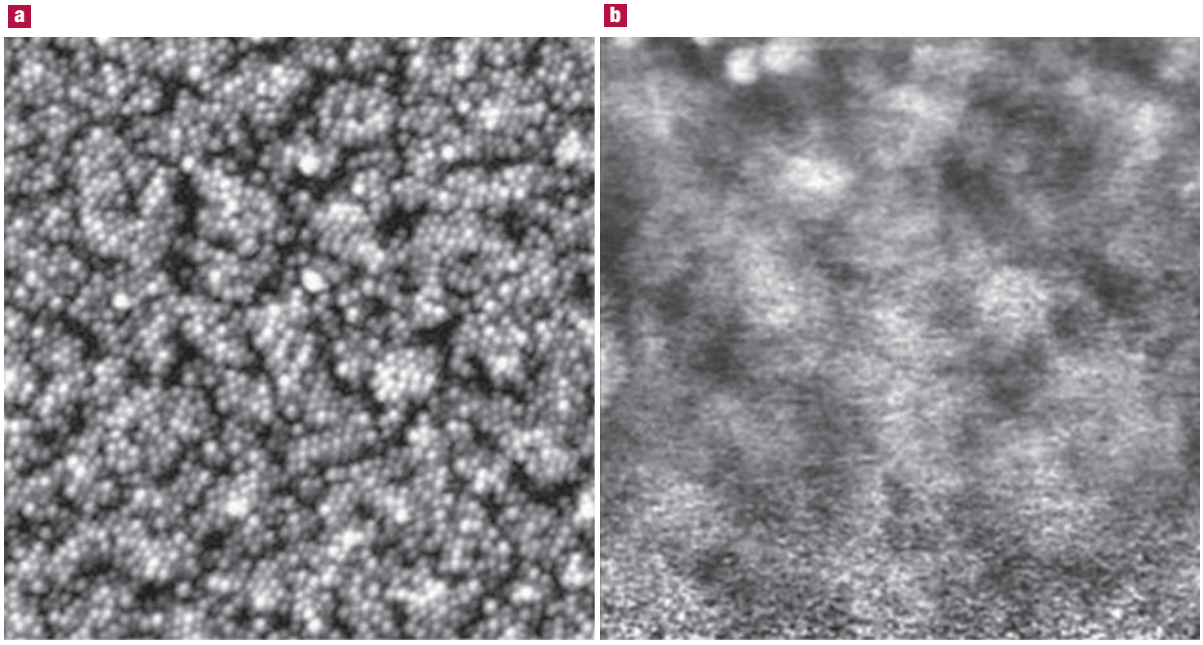

Figure 1 Topography and magnetic structure of a Co nanoparticle compact monolayer. a,**b**, 900 × 900 nm AFM (**a**) and MFM (**b**) images of 12-nm Co nanoparticle 2D assemblies. Vertical scales (from black to white): 0 to 10 nm and 0° to 2°, respectively.

microscopy[18] and spin-polarized scanning-tunnelling microscopy of metallic particles on top of, or embedded in, conductive substrates[19,20]. Magnetization studies of 2D nanoparticle layers may be found in refs 21–24.

An advantage of the applied MFM method, besides its large lateral resolution, is that insulating surfaces can be used. Thus, together with well-coated particles, long-range magnetic interactions mediated by the conduction electrons can virtually be excluded.

In Fig. 1, the physical and magnetic topography of a particle monolayer is observed. The lateral resolution of the atomic force microscope (AFM) image (about 10 nm) is higher than the tip curvature (~50 nm) thanks to the periodicity and regularity of the monolayer.

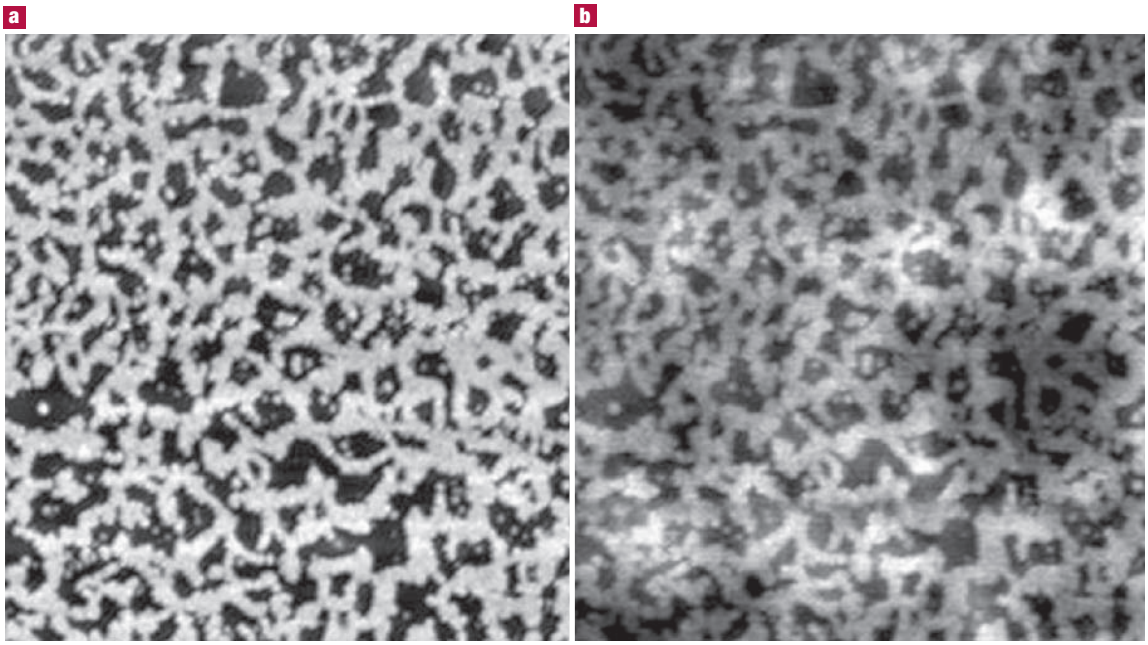

Figure 2 Topography and magnetic structure of a Co nanoparticle incomplete layer. a,**b**, 2 × 2 μm AFM (**a**) and MFM (**b**) images of 12-nm Co nanoparticle 2D assemblies (monolayer). Vertical scales: 10 nm and 2°, respectively.

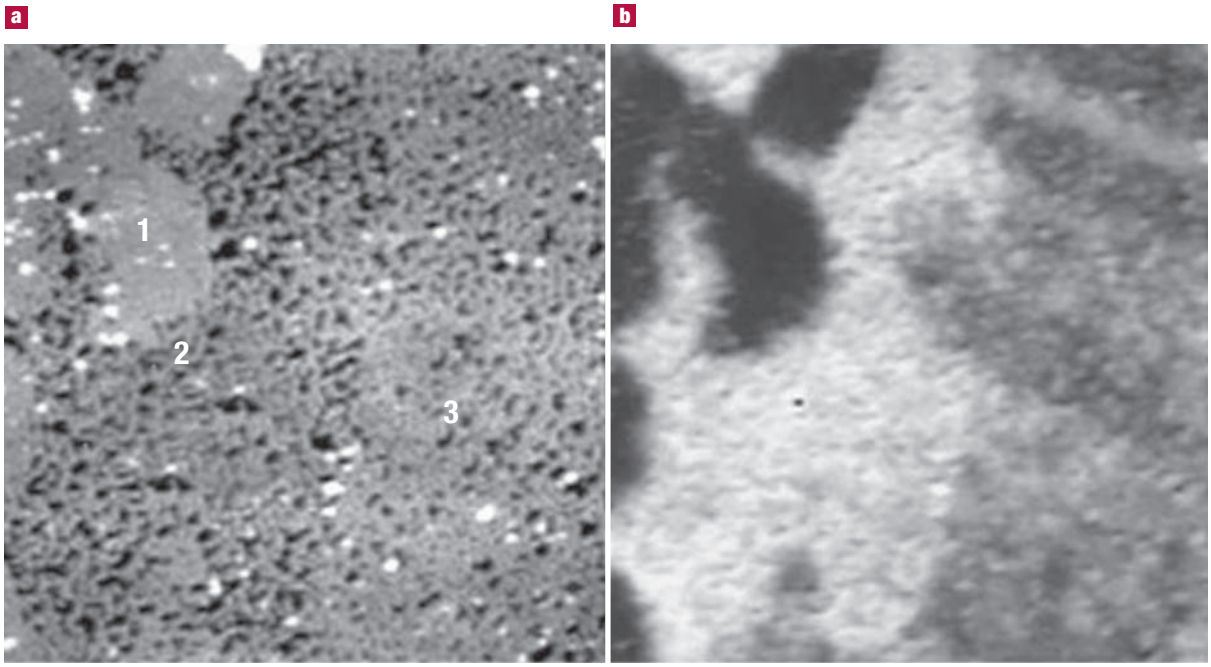

Figure 3 Topography and magnetic structure of a Co nanoparticle monolayer with different particle densities. a,**b**, 5 × 5 μm AFM (**a**) and MFM (**b**) images of 12-nm Co nanoparticle 2D assemblies (monolayer). Vertical scales: 10 nm and 2°, respectively. **1** Corresponds to a compact monolayer as in Fig. 1; **2** to a discontinuous monolayer, as in Fig. 2, and **3** to an intermediate case.

In the MFM image, circular domain-like areas up to few hundred nanometres in size with alternated contrast are observed. The light-coloured areas correspond to repulsion of the tip, whereas darker areas correspond to attraction.

Areas with the same colour are responding similarly to the tip. Despite the different microscopic origin, these magnetic structures are macroscopically similar to the ones observed in weakly ferromagnetic thin films of CoFeAgCu granular alloys[25] or unrecorded hard disks[12].

Less-dense areas also show a similar behaviour (Fig. 2). In these samples, a magnetic structure of correlated areas is also evident. In this case, we are observing continuous magnetized areas, or magnetic percolation, in a highly discontinuous system. In addition, the amplitude of the MFM recorded signal is larger in these network structures than in the compact layer. In this MFM image, the topography is also observed. This is due to the fact that the magnetic dipole is centred in the magnetic particles, and it decays very fast in the absence of particles. Such features are commonly also observed in spin-polarized AFM when probing electric fields[26].

This phenomenon of variation of the amplitude of the magnetic signal as a function of the density of particles—more or less continuous layers—is well observed in Fig. 3 where different nanoparticle density areas display different average magnetic contrast. Zooming into any of those areas reveal the types of magnetic structure and contrast observed in the previous images. Magnetization measurements of a monolayer clearly show the tendency of the magnetization to be in the layer plane. Therefore, as the density of particles increases, the signal (per particle) decreases. In other words, in the less-dense regions, the scanning tip feels a stronger interaction, which causes a higher phase shift. In dense regions, the particle magnetic moment stays in-plane due to dipolar interactions with their neighbours.

To measure this effect, we compare the absolute value of the average magnetic moment as a function of particle density. To have low-density values, we prepared samples in which few particles and small particle agglomerates are far apart, thus non-interacting (Fig. 4). In these samples, the individual particles are not resolved and the agglomerates behave as single dipoles. As previously observed and predicted for single dipoles[15,27], the magnetic signal consists of two blobs of opposite sign, localized at the extremities, and with no magnetic structure in between. The agglomerates are roughly pointing in the same direction; this could be because they are magnetized by the tip during the AFM scan as discussed later.

To perform the calculation of density versus magnetization, we slid a squared window with capacity for 25 particles pixel by pixel in the corresponding AFM and MFM images, comparing density and the absolute value of the average magnetic moment. The results are plotted in Fig. 5. Starting from zero, as the density of particles increases, the signal increases: more magnetic material, more magnetic signal. Beyond a certain point (~0.7 with respect to total coverage), the magnetic signal starts decreasing as the dipolar interactions bring the magnetic dipoles in-plane. A change in the slope indicates the concentration when the dipolar interaction between particles begins to compete successfully with the tip interaction.

Such statistical analysis finds average values, that is, the slope roughly corresponds to the magnetic moment per particle, and it is the change in behaviour that suggests that the system entered a different regime: as the particles become strongly interacting, the magnetic response per particle will decrease due to the stronger particle interactions. The linear regressions give small correlation values (about 0.5). These values are low, but it is generally accepted by statisticians that they represent an x–y correlated system, that is, that there is a trend.

This magnetic percolation is also observed in the hysteresis loops performed on a monolayer of Co nanoparticles. Scanning electron microscope images of the measured sample showed that despite some holes and islands, the sample was primarily a continuous monolayer. The difference between parallel and perpendicular loops (Fig. 6) is typical of a continuous magnetic thin film, where the sample is rapidly

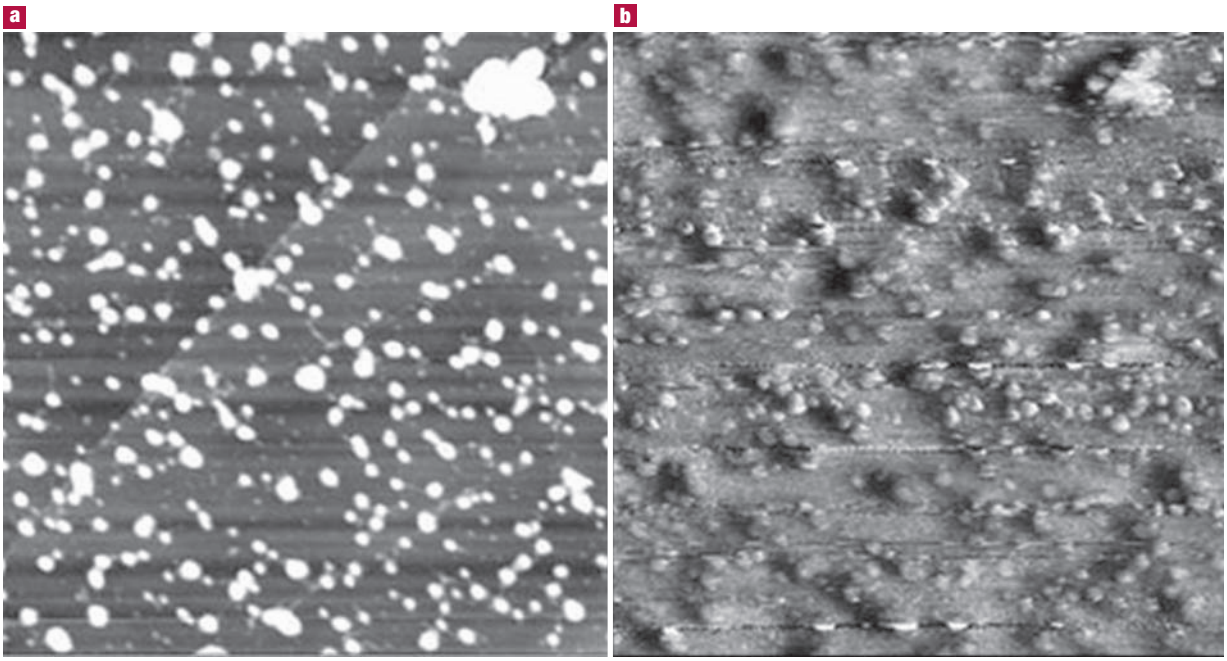

Figure 4 Topography and magnetic structure of Co nanoparticle islands. a,**b**, 3 × 3 μm AFM (**a**) and MFM (**b**) images of 12-nm Co nanoparticles 2D assemblies (individual particles and islands). Vertical scales: 20 nm and 2° respectively.

magnetized when the magnetic field is applied in-plane, whereas much higher fields are required to magnetize the sample in the perpendicular direction[28]. The hysteresis observed at 50 K is only in part due to the particles themselves, as it is larger than that observed in diluted nanoparticle colloids[29], indicating that interactions are partially responsible for the coercivity. In disordered systems, dipolar interactions tend to reduce the coercivity, whereas in ordered systems the dipolar interactions increases it[30]. The softness of the hysteresis loop and the absence of coercivity at room temparature rules out a significant presence of CoO in the magnetic behaviour. In addition, there is no shift after field cooling (to 50 K at 1 T), also indicating the absence of CoO (ref. 31). Furthermore, for small fields, the out-of-plane magnetization is smaller at 50 K than at 300 K, suggesting that at low temperature the magnetic dipolar interactions are stronger, as thermal effects are smaller. Finally, the tendency of the magnetization to be in-plane or out-of-plane can be easily calculated as described elsewhere[28]. In our case, we estimated saturation magnetization: 1,200 e.m.u. cm^{-3}; parallel saturation field: 25.000 Oe; perpendicular saturation field: 27.000 Oe; anisotropy constant: 8.6×10^6 erg cm^{-3} and therefore θ, the angle respect to the plane, 10°.

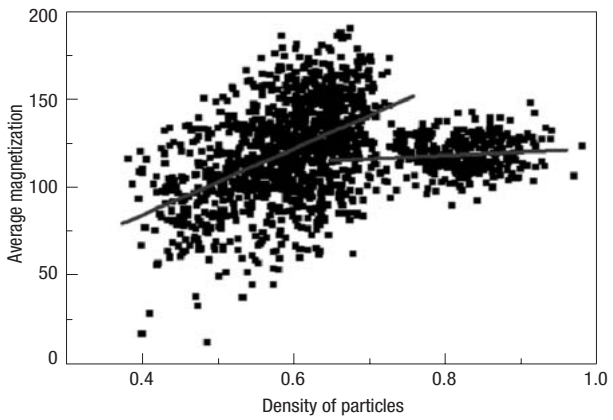

Figure 5 Dependence of the local magnetization as a function of the particle density. Magnetization versus density of particles; the cloud of points on the left correspond to samples as in Fig. 2 and those on the right to samples as in Fig. 1.

In thicker samples (3D), large correlated areas are also observed. However, their stability is weaker than in the previous cases and the magnetic structure is modified as we periodically scan the sample. In Fig. 7, two consecutive MFM images of the same area are shown. Although the topography remained unaltered, the magnetization varied any time that the sample was scanned. Thus, the magnetic structure is combed in the direction of the tip scan, and the signal changes in position and intensity as the sample is consecutively scanned.

A similar result is observed in a larger area where we scan the same area twice and then once again rotating the scan direction by 90°. The topographic structure remains the same, whereas the magnetic structure changes. It seems that the 3D structures are more unstable, probably thanks to the extra degree of freedom that exist in the third dimension, that is, the system has more possible final states and an increased instability. Consequently, the observed structure depends on the scanning rate. Unfortunately, this rate cannot be freely modified without losing optimal imaging conditions.

One has also to bear in mind that before the MFM scan, where the tip approaches the sample at approximately 50 nm, the tip is scanned at 5 nm to record the surface structure. Thus, the sensing magnet of the tip is first scanned very close to the particles in what remains a write (AFM)–read (MFM) process.

We studied the magnetic response of assemblies of nanoparticles consisting of a core of Co surrounded by a 1-nm shell of oleic acid. The Co particles are spherical (no shape anisotropy) and with epsilon

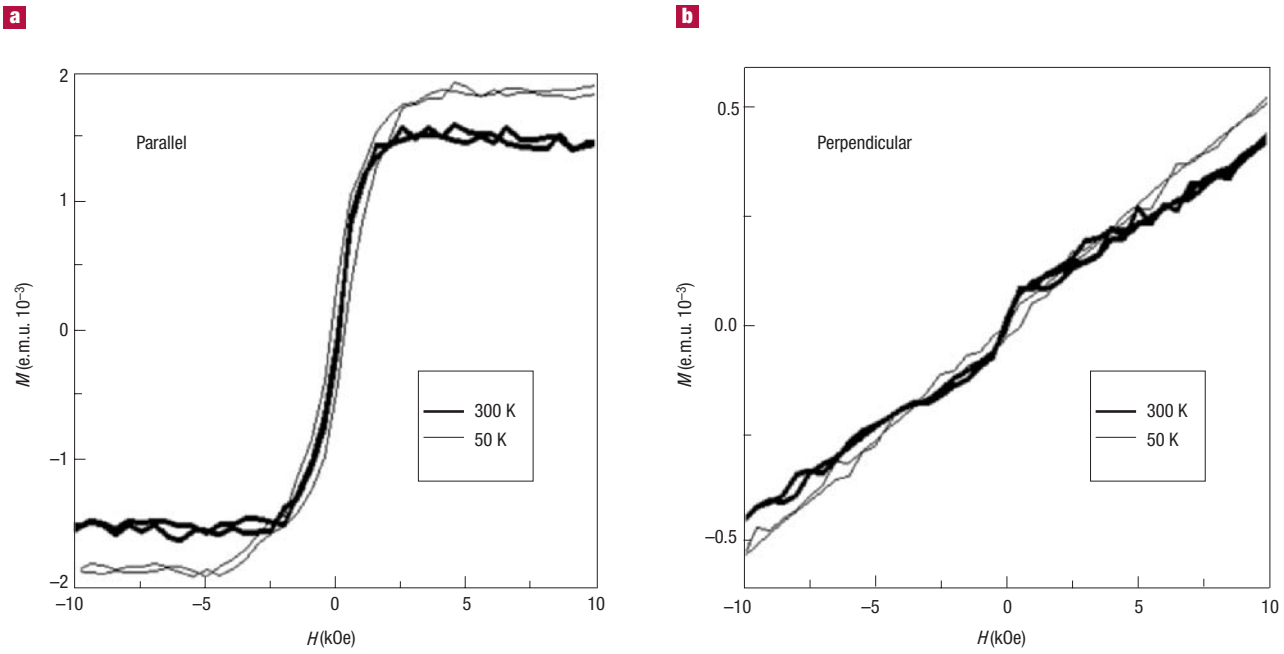

Figure 6 Magnetization measurements as a function of field orientation and temperature. a, Parallel and **b**, perpendicular hysteresis loops at 300 K and 50 K of 12-nm Co monolayer.

(cubic) crystal anisotropy (six easy magnetization axes). ε-Co consists of a complex cubic primitive structure ($P4132$, $a = 6.09$ Å), isotypic relative to the beta phase of manganese, with 20 atoms present in the elemental cell[32]. In these assemblies, dipolar interactions are strong, as they are systems of strong magnetic moment and low and degenerated anisotropy. The magnetization measurements of 2D self-assemblies suggest a collective behaviour where groups of particles have their moments (or fraction of it) parallel, and which will rotate together towards an applied field. This behaviour, previously measured with a macroscopic probe (superconducting interference device (SQUID) magnetometry) was here verified with a local probe (MFM), where correlated areas (same contrast) of a few tens of nanoparticles in diameter are observed. The change in behaviour of the magnetization versus particle density indicates that in dense areas a collective behaviour is set.

Thus, in addition to the difficulty of finding the smallest, yet stable, bits[33,34], two problems seem to arise when maximizing recording capacity: dipolar interactions are not negligible when the particle distance is smaller than few nanometres; and due to the nature of the magnetic fields and dipolar interactions, in very high dipole density

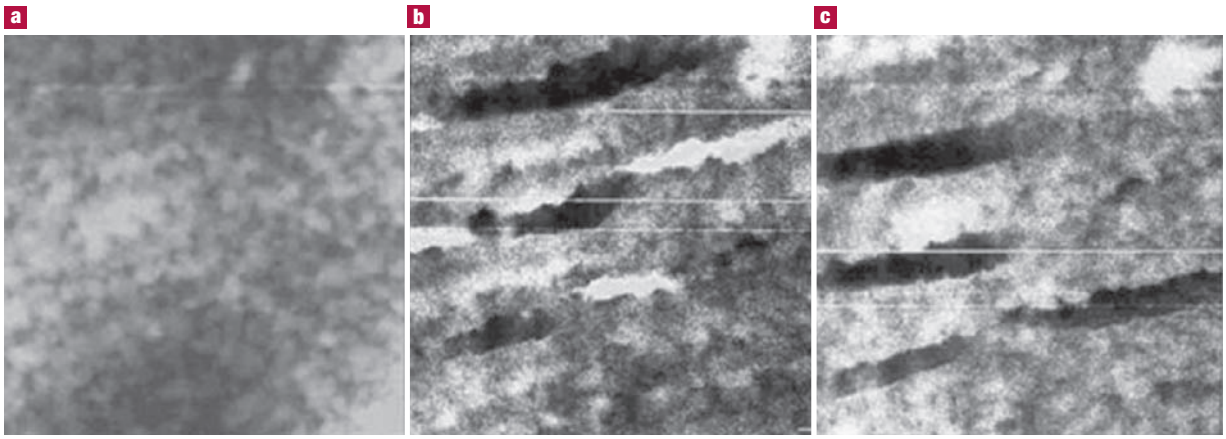

Figure 7 Topography and magnetic structure of a Co nanoparticle multilayer. a,**b**, 8 × 8 mm AFM (**a**) and MFM (**b**,**c**) images of two consecutive scans on exactly the same area. Vertical scales: 200 nm and 1°, respectively. The scan direction was left to right. These samples present high metastability and a variety of remanent in-plane and out-of-plane microstructures can be achieved as a function of the magnetic history. The horizontal lines on these figures are artefacts from the microscope probe signal.

the write–read head would have trouble dealing with individual bits. Thus, lower-density monolayers (magnetic particles further apart, by increasing the coating, patterning the substrate and so on) would be needed to independently read and write one bit per particle. Otherwise, high anisotropy particles (normally at the expense of the magnetic dipole intensity) or pinning centres (to avoid the propagation of interactions) would be needed to decrease the effects of dipolar interactions. In other scenarios, the perturbable stability of the long-range order may be useful for sensing applications.

METHODS

MAGNETIC PARTICLES

Spherical ε-cobalt nanoparticles (12 nm in diameter) coated with oleic acid were synthesised[35,36]. We chose particles of 12 nm diameter to be able to have a large enough magnetic signal at room temperature. 2D self-assemblies of smaller particles did not give any MFM signal.

MFM SAMPLE PREPARATION

12-nm particles give an MFM signal, but their magnetic interactions are strong, so they tend to make closed loops and mixtures of chains and layers when deposited[35]. Thus, to obtain a monolayer we had to attach them chemically to a substrate[37]. In detail, single-crystal silicon wafers of the (110) or the (111) orientation were cut into small pieces. The pieces were then cleaned by immersion in piranha (30% v/v H_2O_2, 70% v/v concentrated H_2SO_4) at 110 °C for 30 minutes. The silicon was then copiously rinsed with 18.2 MΩ cm H_2O and then absolute ethanol. Subsequently, the silicon was immediately plunged into a freshly mixed solution (2% by volume) of 3-[2-(2-aminoethylamino)ethylamino]propyl-trimethoxysilane (Fluka) in 95% ethanol (balance water). After two minutes, the pieces were plunged into absolute ethanol and copiously rinsed with ethanol to remove any traces of free silane. The silicon pieces were baked in an oven at 130 °C for 20 minutes or put under vacuum (10^{-7} torr) to complete the silanization by removing water. We thus obtained an amino-functionalized surface. The silanized pieces were brought into an argon drybox and soaked in concentrated solutions of nanoparticles in 1,2-dichlorobenzene for 12–24 hours. The pieces were then taken out of the solution and rinsed with 2–3 ml of 1,2-dichlorobenzene to remove any excess nanoparticles. They were then dried under dry nitrogen.

Two other types of samples were also prepared: (i) We heated a piece of highly oriented pyrolytic graphite to 50 °C and deposited a drop of dilute solution (clear tea colour, 10^{14} particles per ml in toluene, as opposed to 10^{16} particles per ml in *o*-dichlorobenzene in the original solution). Rapid evaporation resulted in individual particles being present on the surface, as well as aggregates. (ii) Multilayers (about 20 particles thick) were prepared by spin-coating a MeOH-desestabilized solution against a Teflon flat substrate. These particles re-dissolve after the microscopy experiments, indicating that there is no loss of oleic acid.

MFM

A Nanoscope III (Digital instruments, Santa barbara, California) was used. The magnetic clamps were removed and the samples stuck with double-sided tape to the stage. Soft tapping conditions were used to avoid particle displacements, surfactant indentation, or height artefacts[38]. Lift mode while tapping was used to record the magnetic signal using the phase-detection mode. We used high magnetic moment (thicker CoCr coating) MFM tips. To improve imaging, the drive amplitudes and the feedback of the topological (AFM) and the lift (MFM) scans were decoupled so they could be tuned separately. We combined higher lift height (100–200 nm) with high drive amplitude (up to 17,000 mV), which results in an improved signal-to-noise ratio. Thus, despite a reduction of intensity of the signal, the magnetic features were better resolved[39]. Images were recorded at slow scan rates of 10 μm min^{-1}. To ensure that we were only detecting a magnetic signal, we also imaged gold nanoparticle assemblies (10 nm) on a mica substrate in the same conditions. As another control, we also performed imaging in MFM mode with a non-magnetic tip. In addition, we were careful that the contrast in the MFM image was at the same position in the trace and retrace scans. This indicates that the contrast in the phase image is not due to the sudden change in topography, or other artefacts. Lateral resolution in standard MFM is about 50 nm.

MAGNETOMETRY

A SQUID magnetometer (MPMS, Quantum Design) was used to record the magnetic signal (in-plane and out-of-plane) of a Co nanoparticle monolayer. To check if the particles were oxidized, and the implication of that oxidation on the magnetic behaviour, we performed hysteresis loops after 1-T field cooling at 50 K, a temperature lower than the CoO Neel temperature (corresponding to the ordering of the antiferromagnetic phase). CoO–Co coupling would result in either exchange coupling, which would increase the anisotropy and thus the coercivity, and/or exchange bias, which would induce an *x*-shift in the loops after field cooling[31].

IMAGE ANALYSIS

To analyse magnetization versus density of particles per unit area, we wrote a program on C++ based on the analysis of wavelets[40]. To compare topography (AFM) and magnetic structure (MFM), and to have good statistics we chose square windows that can contain up to 25 particles (60 × 60 nm). With a local threshold we determined the number of particles per window, and then we slid this window pixel by pixel, comparing density and the absolute value of the average magnetic moment. We obtain thus about 25,000 window pairs, and pairs of points, per image. Density values of one correspond to a compact triangular nanoparticle assembly.

Received 6 December 2003; accepted 10 February 2004; published 28 March 2004.

References

1. Seul, M. & Andelman, D. Domain shapes and patterns: the phenomenology of modulated phases. *Science* **267,** 476–483 (1995).
2. Vidal Russell, E. & Israeloff, N. E. Direct observation of molecular cooperativity near the glass transition. *Nature* **408,** 695–698 (2000).
3. Young, A. P. *Spin Glasses and Random Fields* (World Scientific, Singapore, 1998).
4. Parisi, G. Complex systems: a physicist's viewpoint. *Physica A* **263,** 557–564 (1999).
5. Sun, S. & Murray, C. B. Synthesis of monodisperse cobalt nanocrystals and their assembly into magnetic superlattices (invited). *J. Appl. Phys.* **85,** 4325–4390 (1999).
6. Sun, S., Murray, C. B., Weller, D., Folks, L. & Moser, A. Monodisperse FePt nanoparticles and ferromagnetic FePt nanocrystal superlattices. *Science* **287,** 1989–1992 (2000).
7. Weiss, J. Simulation of quasi-two-dimensional dipolar systems *J. Phys. Condens. Matter* **15,** S1471–S1495 (2003).
8. Puntes, V. F., Alivisatos, A. P. & Krishnan, K. Synthesis, self-assembly, and magnetic behavior of a two-dimensional superlattice of single-crystal ε-Co nanoparticles. *Appl. Phys. Lett.* **78,** 2187–2199 (2001).
9. Porthun, S., Abelmann, L. & Lodder, C. Magnetic force microscopy of thin film media for high-density magnetic recording. *J. Magn. Magn. Mater.* **182,** 238–273 (1998).
10. Folks, L. & Woodward, R. C. The use of MFM for investigating domain structures in modern permanent magnet materials. *J. Magn. Magn. Mater.* **190,** 28–41 (1998).
11. Babcock, K. L., Elings, V. B., Shi, J., Awschalom, D. D. & Dugas, M. Field-dependence of microscopic probes in magnetic force microscopy. *Appl. Phys. Lett.* **69,** 705–707 (1996).
12. Vellekoop, S. J. L., Abelmann, L., Porthun, S., Lodder, J. C. & Miles, J. J. Calculation of playback signals from MFM images using transfer functions. *J. Magn. Magn. Mater.* **193,** 474–478 (1999).
13. Kleiber, M. *et al.* Magnetization switching of submicrometer Co dots induced by a magnetic force microscope tip. *Phys. Rev. B* **58,** 5563–5567 (1998).
14. Gider, S. *et al.* Imaging and magnetometry of switching in nanometer-scale iron particles. *Appl. Phys. Lett.* **69,** 3269–3271 (1996).
15. Proksch, R. B. *et al.* MFM of the submicron magnetic assembly in magnetotactic bacterium. *Appl. Phys. Lett.* **66,** 2582–2584 (1995).
16. Sun, S. *et al.* Polymer mediated self-assembly of magnetic nanoparticles. *J. Am. Chem. Soc.* **124,** 2884–2885 (2002).
17. Rasa, M., Kuipers, B. W. M. & Philipse, A. P. Atomic force microscopy and magnetic force microscopy study of model colloids. *J. Colloid Interface Sci.* **250,** 303–315 (2002).
18. Majetich, S. A. & Jin, Y. Magnetization directions of individual nanoparticles. *Science* **284,** 470–473 (1999).
19. Yamasaki, A., Wulfhekel, W., Hertel, R. & Kirschner, J. Direct observation of the single-domain limit of Fe nanomagnets by spin-polarized scanning tunneling spectroscopy. *Phys. Rev. Lett.* **91,** 127201 (2003).
20. Kubetzka, A., Bode, M., Pietzsch, O. & Wiesendanger, R. Spin-polarized scanning tunneliung microscopy with antiferromagnetic probe tips. *Phys. Rev. Lett.* **88,** 057201 (2002).
21. Respaud, M. *et al.* Surface effects on the magnetic properties of ultrafine cobalt particles. *Phys. Rev. B* **57,** 2925–2935 (1998).
22. Binns, C., Maher, M. J., Pankhurst, Q. A., Kechrakos, D. & Trohidou, K. N. Magnetic behavior of nanostructured films assembled from preformed Fe clusters embedded in Ag. *Phys. Rev. B* **66,** 184413 (2002).
23. Padovani, S., Chado, I., Scheurer, F. & Bucher, J. P. Transition from zero-dimensional superparamagnetism to two-dimensional ferromagnetism of Co clusters on Au. *Phys. Rev. B* **59,** 11887–11891 (1999).
24. Russier, V., Petit, C. & Pileni, M. P. Hysteresis curve of magnetic nanocrystals monolayers: influence of the structure. *J. Appl. Phys.* **93,** 10001–10010 (2003).
25. Franco-Puntes, V., Batlle, X. & Labarta, A. Evidence of domain wall scattering in thin films of granular CoFe-AgCu. *European Phys. J. B* **17,** 43–51 (2000).
26. Hu, J., Xiao, X.-D., Ogletree, D. F. & Salmeron, M. Imaging the condensation and evaporation of molecularly thin films of water with nanometer resolution. *Science* **269,** 267–269 (1995).
27. Fredkin, D. R. & Koehler, T. R. Micromagnetic modeling of permalloy particles: thickness effects. *IEEE Trans. Magn.* **27,** 4763–4765 (1991).
28. Xiao, J. Q., Chien, C. L. & Gavrin, A. Observation of perpendicular anisotropy in granular magnetic solids. *J. Appl. Phys.* **79,** 5309–5311 (1997).
29. Puntes, V. F. & Krishnan, K. Synthesis, structural order and magnetic behavior of self-assembled epsilon-Co nanocrystal arrays. *IEEE Trans. Magn.* **37,** 2210–2212 (2001).
30. Lederman, M., Fredkin, D. R., O'Barr, R., Schultz, S. & Ozaki, M. Measurement of thermal switching of the magnetization of single domain particles (invited). *J. Appl. Phys.* **75,** 6217–6222 (1994).
31. Peng, D. L., Sumiyama, K., Hihara, T. & Yamamuro, S. Enhancement of magnetic coercivity and macroscopic quantum tunneling in monodispersed Co/CoO cluster assemblies. *Appl. Phys. Lett.* **75,** 3856–3858 (1999).
32. Dinega, D. P. & Bawendi, M. G. A Solution-phase chemical approach to a new crystal structure of cobalt. *Angew. Chem. Intl Edn Engl.* **38,** 1788–1791 (1999).
33. Skumryev, V. *et al.* Beating the superparamagnetic limit with exchange bias. *Nature* **423,** 850–853 (2003).
34. Gambardella, P. *et al.* Giant magnetic anisotropy of single cobalt atoms and nanoparticles. *Science* **300,** 1130–1132 (2003).
35. Puntes, V. F., Krishnan, K. & Alivisatos, P. Nanocrystals size and shape control: the case of Co. *Science* **291,** 2115–2117 (2001).
36. Puntes, V. F., Zanchet, D., Erdonmez, C. & Alivisatos, A. P. Synthesis of hcp-Co nanodisks. *J. Am. Chem. Soc.* **124,** 12874–12880 (2002).
37. Colvin, V. L., Goldstein, A. N. & Alivisatos, A. P. Semiconductor nanocrystals covalently bound to metal surfaces using self assembled monolayers. *J. Am. Chem. Soc.* **114,** 5221–5230 (1992).
38. Ebenstein, Y., Nahum, E. & Banin, U. Tapping mode atomic force microscopy for nanoparticle sizing: Tip-sample interaction effects. *Nano Lett.* **2,** 945–950 (2002).
39. Kebe, Th. & Carl, A. Calibration of magnetic force microscopy tips by using nanoscale current-carrying parallel wires. *J. App. Phys.* **95,** 775–792 (2004).
40. Graps, A. An introduction to wavelets. *IEEE Comput. Sci. Eng.* **2,** 50–61 (1995).

Acknowledgements

We thank the technical help and scientific discussion with Peter Nilson from Digital Instruments and Antonio Turiel from the University of Barcelona. Funding came from SEUID MAT2003-01124, DURSI 2001SGR00066, NIH 1 R01 RR-14891-01 and DE-AC03-76SF00098.

Correspondence and requests for materials should be addressed to V. F. P.

Competing financial interests

The authors declare that they have no competing financial interests.